A Comparison of Neonatal and Adult Fibrin Clot Properties Between Porcine and Human Plasma

Kimberly A. Nellenbach, BS[1,2], **Seema Nandi, BS**[1,2], **Alexander Kyu**[1], **Supriya Sivadanam, BS**[1], **Nina A. Guzzetta, MD FAAP**[3], **Ashley C. Brown, PhD**[1,2]

[1]Joint Department of Biomedical Engineering, North Carolina State University and The University of North Carolina at Chapel Hill, Raleigh, NC 27695, USA

[2]Comparative Medicine Institute, North Carolina State University, Raleigh, NC 27695, USA

[3]Department of Anesthesiology, Emory University School of Medicine and Children's Healthcare of Atlanta, Atlanta, GA, 30322, USA

Abstract

Background: Recent studies suggest that adult specific treatment options for fibrinogen replacement during bleeding may be less effective in neonates. This is likely due to structural and functional differences found in the fibrin network between adults and neonates. In this investigation, we performed a comparative laboratory-based study between immature and adult human and porcine plasma samples in order to determine if piglets are an appropriate animal model of neonatal coagulopathy.

Methods: Adult and neonatal human and porcine plasma samples were collected from the Children's Hospital of Atlanta and North Carolina State University College of Veterinary Medicine, respectively. Clots were formed for analysis, and fibrinogen concentration was quantified. Structure was examined through confocal microscopy and cryogenic scanning electron microscopy. Function was assessed through atomic force microscopy nanoindentation and clotting and fibrinolysis assays. Lastly, novel hemostatic therapies were applied to neonatal porcine samples to simulate treatment.

Results: All sample groups had similar plasma fibrinogen concentrations. Neonatal porcine and human plasma clots were less branched with lower fiber densities than the dense and highly branched networks seen in adult human and porcine clots. Neonatal porcine and human clots had faster degradation rates and lower clot stiffness values than adult clots (stiffness (kPa) means +/− SD: neonatal human: 1.62 +/− 0.18 kPa vs. adult human: 4.30 +/− 0.95 kPa $P = 0.016$; neonatal pig 1.14+/− 1.1 vs adult pigs: 4.34 +/− 0.96 kPa, $P = 0.015$). The addition of hemostatic therapies to neonatal porcine samples enhanced clot formation.

Corresponding Author: Ashley C. Brown, PhD, Biomedical Partnership Center Building, 1001 William Moore Dr; Office 26, Raleigh, NC 27606, 919-513-8231, aecarso2@ncsu.edu.

Clinical Trial Number: Not applicable

Conflicts of Interest: The authors declare no competing acterests.

Conclusions: We identified similar age-related patterns in structure, mechanical, and degradation properties between adults and neonates in porcine and human samples. These findings suggest that piglets are an appropriate pre-clinical model of neonatal coagulopathy. We also show the feasibility of *in vitro* model application through by analyzing novel hemostatic therapies when applied to dilute neonatal porcine plasma.

Summary Statement:

No preclinical models of neonatal coagulopathy exist. Here we validate a preclinical porcine model by comparing structural and functional properties of adult and neonatal porcine and human clots in vitro.

Introduction:

The coagulation system is immature at birth and matures throughout the first year of life[1-3]. Physiologically, healthy newborns show excellent hemostasis, but when compromised, such as critically ill neonates undergoing major surgery with cardiopulmonary bypass (CPB) or extracorporeal membrane oxygenation, their neonatal hemostatic immaturity can have critical clinical implications[2,4], and is a contributory factor to serious post-operative bleeding. The current standard-of-care treatment for bleeding in neonates is the transfusion of adult blood products including packed red blood cells, platelets, cryoprecipitate (fibrinogen component) and fresh frozen plasma[4-6]. However, this treatment has inconsistent efficacy and the use of allogenic blood products is associated with multiple infectious and non-infectious risks[5]. Additionally, our recent studies demonstrate that one of the essential clotting proteins, fibrinogen, is structurally and functionally distinct between neonates and adults. Moreover, when mixed together to simulate transfusion of cryoprecipitate (adult fibrinogen component), the resulting fibrin networks are structurally and functionally distinct compared to those formed solely from native neonatal fibrinogen[7].

Recent investigations in developmental hemostasis indicate that neonatal fibrinogen exists in a fetal form until maturation and that its replacement with adult fibrinogen following CPB may lead to inconsistent efficacy in treating post-CPB bleeding[7-9]. Developing neonatal specific treatment strategies to mitigate bleeding, especially during or after major surgery, could potentially improve outcomes in this challenging patient population. Unfortunately, there has been no validation of the observed differences in neonatal versus adult fibrin structure in animal models. Establishing a validated animal model would facilitate the preclinical analysis of neonatal specific hemostatic therapies prior to the implementation of clinical trials.

Here, we performed a comparative study between neonatal and adult human and porcine plasma samples to determine if piglets accurately reflect the maturation of human fibrinogen. Pigs represent an appealing model to use in translational medicine due to their anatomical and physiological similarities to humans particularly in regard to the hemostatic system[10,11,12,13]. Thus we hypothesize that pigs possess age-related differences in fibrinogen that parallel those identified in humans[14]. The primary objective of this study was to validate the fibrin network in piglets as an appropriate *in vitro* animal model for that of human neonates. We accomplish this by characterizing fibrin network parameters formed

from plasma collected from neonatal and adult humans and pigs. Our second objective was to analyze the *in vitro* effect of several novel and commercially relevant pro-coagulant therapies on the fibrin network properties of neonatal porcine samples. We utilized a model of post-CPB dilutional coagulopathy because procoagulant therapies are currently being used off-label as rescue agents to control bleeding after CPB in neonates when conventional blood transfusions fail[5,15,16]. Also, our previous studies demonstrate that the *ex vivo* addition of pro-coagulant therapies to post-CPB plasma from human neonates enhances fibrin clot properties[17-20]. We hypothesize that the *in vitro* addition of these hemostatic therapies to neonatal porcine samples will similarly augment plasma fibrin clot properties. If confirmed, piglets could serve as a suitable and much needed preclinical model for evaluating neonatal specific hemostatic therapies.

Materials and Methods:

Human plasma collection:

After IRB approval and parental informed written consent, blood samples were collected from 10 human neonates (less than 30 days of age) undergoing corrective cardiac surgery with CPB at the Children's Hospital of Atlanta. All samples were collected from an arterial line placed after the induction of anesthesia and prior to surgical incision and CPB. Samples were centrifuged immediately to yield platelet poor plasma and stored at −80 until use. All patient samples were deidentified prior to sample transfer to North Carolina State University. Pooled adult human platelet poor plasma was obtained from the New York Blood Center.

Porcine plasma collection:

Blood was collected from 8 1 year old female Yorkshire pigs and 8-week-old Yorkshire piglets prior to planned surgical procedures at North Carolina State University's School of Veterinary Medicine, (Raleigh, NC, USA) through the tissue sharing program. Porcine ages and sample size were selected in order to minimize animal use. For this study, we utilized samples from pigs that were readily available in sufficient numbers. All samples were collected via jugular venous puncture after the induction of anesthesia and prior to surgical incision. Samples were centrifuged immediately to obtain platelet poor plasma and stored at −80 °C until use.

Quantification and isolation of fibrinogen from platelet poor plasma:

Quantification of fibrinogen concentration was achieved via enzyme linked immunosorbent assays (ELISA; Abcam, USA) with human and porcine protein quantification kits. Isolated fibrinogen was utilized for clottability assays. Fibrinogen was purified from plasma via an ethanol precipitation reaction. Briefly, ethanol (70% volume) was added to 4°C plasma in a 4:1 ratio (plasma:ethanol) and cooled on ice for 20 min. The solution was then centrifuged for 15 min at 4°C. The supernatant plasma was removed and the resulting pellet was heated in a 37°C water bath. A buffer consisting of 20 mM sodium citrate was added until the pellet was fully dissolved. Protein concentration was determined via absorbance readings at 280 nm using a Nanodrop Microvolume UV-Vis Spectrophotometer (ThermoFisher Scientific, USA).

Analysis of fibrinogen clottability:

Percentage of total fibrinogen clottability was determined by a protein quantification based assay which measures the protein content in the clot liquor (soluble portion of clot sample) remaining after polymerization. Clots totaling 50 µl were formed with purified fibrinogen at a concentration of 2.5 mg/mL, HEPES buffer (5 mM calcium, 7.4 pH) and were polymerized with the initiation of 0.5 U/mL thrombin. Five µl aliquots were taken before and after a one hour polymerization period and quantified via NanoOrange Protein Quantification Kit (Invitrogen, USA). Alternately, 50 µl plasma clots were formed with 0.5 U/mL thrombin and quantification was conducted via ELISA for pig or human fibrinogen (Abcam, USA). Percent of clottable fibrinogen was determined as: [(initial soluble protein)-(soluble protein in clot liquor)]/(initial soluble protein) x 100[21].

Analysis of clot architecture:

Confocal microscopy was utilized to examine clot structure from neonatal and adult human and porcine plasma samples. Clots consisting of 90% plasma by volume were polymerized with 0.1, 0.25, or 0.5 U/ml of human thrombin (Enzyme Research Labs, USA), and 10 µg/ml of Alexa-Flour 488 labeled fibrinogen for visualization. Clots were formed between a glass slide and coverslip and allowed to polymerize for two hours prior to imaging. A Zeiss Laser Scanning Microscope (LSM 710, Zeiss Inc., USA) at a magnification of 63x was utilized for imaging and a minimum of three random 5.06 µm z-stacks were acquired per clot. ImageJ software was used to create 3D projections from z-stacks. Clot fiber density was determined from the ratio of black (fiber) over white (background) pixels in each image. Fibrin clot alignment was quantified with a custom matlab algorithm previously utilized in Brown et al.[22,7]. An alignment index was determined from the fraction of fibers aligned within +/− 20 degrees of a preferred fiber alignment normalized to random distribution of oriented fibers. A greater alignment index corresponds to a higher percentage of fibers aligned near the preferred fiber alignment. Alignment index values range from 1.0 to 4.55. Alignment analysis was conducted for each image in the z stack and averaged together. Clot structure in porcine samples was additionally assessed with cryogenic scanning electron microscopy to examine three-dimensional clot architecture. Again, 50 µl plasma clots were formed with 0.5 U/mL thrombin and allowed to polymerize for two hours prior to imaging. Clots were rapidly frozen in sub-cooled liquid nitrogen and imaged at 2,500x. Three clots were imaged per group and three random images were taken per clot.

Analysis of clot stiffness:

Clot mechanical properties were examined using atomic force microscopy (Asylum MFP3D-Bio, Asylum Research, USA) operated in force contact mode to obtain stiffness values. Plasma clots formed with 0.5 U/mL human thrombin were polymerized directly on a glass slide 1.5 hours prior to force measurements. Standard silicon nitride cantilevers with a particle diameter of 1.98 µm (Nanoandmore, USA) were utilized. Force maps of 20 µm X 20 µm dimensions were collected on each clot and fit with a Hertz model to obtain the elastic modulus. A minimum of two random force maps were generated per clot with the average elastic modulus reported.

Analysis of clot degradation:

Fibrinolysis was assessed for neonatal and adult human and porcine samples. A custom microfluidics based assay adapted from Brown et al. was utilized to analyze degradation rates for all sample groups[17,18]. A polydimethylsiloxane (Dow Corning, USA) device consisting of a clot reservoir with a perpendicular lying channel was constructed via casting in an acrylic mold. After curing for 24 hours, the device was plasma treated and bonded to a glass slide to create a sealed channel. Clots were formed from plasma and 10% Alexa-Flour 488–labeled adult fibrinogen was added for visualization. Polymerization was initiated with the addition of 0.5 U/ml of thrombin, and 25 μl of the clot solution was immediately injected into the clot reservoir. After polymerizing for two hours, the device was mounted on an EVOS FL Auto microscope (Life Technologies, USA) for imaging. A plasmin solution (0.01 mg/ml plasmin in HEPES buffer) (Human Plasmin, Enzyme Research Laboratories, USA) was injected into a channel inlet, and the clot was imaged every 10 min for 12 hours. ImageJ (National Institutes of Health, USA) was used to determine rate of clot degradation by comparing the first and final images and measuring distance along a perpendicular line to the clot boundary. Clot degradation rates were expressed as the distance the clot boundary traveled divided by 12 hours.

Analysis of procoagulants in a hemodilution model of coagulopathy:

To mimic the reduction of clotting factors seen after CPB, porcine plasma was diluted for all subsequent assays. Initial fibrinogen levels of eight week old porcine plasma were determined via ELISA (Pig Fibrinogen ELISA, Abcam, USA). For all structural and functional assays, plasma was diluted to a final concentration of 1.5 mg/mL to match the fibrinogen concentration in human neonates post-CPB observed in our previous studies[7]. The following procoagulants were added to the dilute neonatal plasma to simulate treatment after CPB: recombinant activated factor VII (rFVIIa; Novo Nordisk Inc., Plainsboro, New Jersey), Factor eight inhibitor b bypassing activity (FEIBA; Shire US Inc., Lexington, MA), RiaSTAP Fibrinogen Concentrate (CSL Behring, Marburg, Germany), and novel synthetic platelet-like particles developed by our group. We chose the above therapies because factor VIIa, FEIBA, RiaSTAP have been used off-label as rescue agents to control bleeding after CPB in neonates when the standard-of-care fails[5,15,16]. Additionally, FEIBA, a prothrombin complex concentrate, was utilized in this study because of its use at our clinical institution. However, it should be noted that Kcentra is an additional prothrombin complex concentrate that is also used clinically. The synthetic platelet-like particles utilized for these studies have previously been shown to enhance human neonatal fibrin clot properties *in vitro*[17]. Diluted porcine plasma was used to form 50 μl clots with 0.5 U/mL thrombin in the presence of 0.05 mg/mL factor VIIa, 0.3 U/mL FEIBA, 0.89 mg/mL RiaSTAP, or 0.5 mg/mL PLPs. Factor VIIa, RiaSTAP, and FEIBA concentrations were chosen to reflect a clinically utilized dose, while the platelet-like particle concentration was chosen based off of optimized experiments previously conducted by our group[19]. Synthetic platelet-like-particles were synthesized and characterized as previously described by covalently coupling highly deformable ultralow crosslinked microgels to a fibrin-specific antibody[17]. Ultralow crosslinked poly(N-isopropylacrylamide-co-acrylic acid) microgels were synthesized via a precipitation polymerization reaction and characterized via atomic force microscopy dry imaging to determine particle deformability (Supplemental Figure 1). Platelet-like particles were

created by covalently coupling microgels to a sheep anti-human fibrin fragment E polyclonal IgG antibody using N-(3Dimethylaminopropyl)-N'-ethylcarbodiimide hydrochloride/N-hydroxysuccinimide chemistry. Particles were purified via dialysis for 72 hours, lyophilized, and re-suspended at 10 mg/mL. For analysis of clot structure in the presence and absence of hemostatic therapies, confocal microscopy was utilized as described above. To examine clottability of diluted plasma with and without the addition of procoagulant agents, 50 μl clots were formed and protein quantified before and after polymerization. Fibrinogen was quantified via ELISA (Pig Fibrinogen ELISA, Abcam, USA) and clottability was calculated as described above.

Statistical Analysis:

All statistical analyses were performed with a repeated measures one-way ANOVA test using Graphpad Prism Software (USA) with a Tukey's posthoc analysis with a 95% confidence interval. Analysis was performed between sample groups. Statistical significance was achieved for $p < 0.05$. No a priori statistical power calculation was conducted. Data is defined as interval and is presented as average +/− standard deviation. Outlier tests were performed on all datasets prior to graph creation and statistical analysis. No outliers were identified. There was no missing data.

Results:

Quantification of plasma fibrinogen levels:

Fibrinogen concentrations were quantified across age groups and species (Figure 1). We observed similar values of fibrinogen across species and age groups that is consistent with previous studies (neonatal humans: 246 +/− 90 mg/dL, neonatal pigs: 295 +/− 89 mg/dL, adult humans: 265 +/− 116 mg/dL, adult pigs: 346 +/− 59 mg/dL; neonatal humans vs. adult humans: P=0.993, neonatal pigs vs. adult pigs: P=0.898, neonatal human vs. neonatal pigs: P= 0.909, adult human vs. adult pigs: P=0.705). Additionally, porcine fibrinogen concentrations were within normal human ranges of 200-450mg/dL[23].

Analysis of fibrinogen clottability:

To compare functional ability of fibrinogen across species and age groups, clottability of the purified protein was quantified (Figure 2). We demonstrate that neonatal samples had statistically significant lower clottability across species compared to their adult counterparts (neonatal humans: 29 +/− 16 %, neonatal pigs: 25 +/− 17 %, adult humans: 78 +/− 17 %, adult pigs: 81 +/− 21%; neonatal humans vs. adult humans: P= 0.010, neonatal pigs vs. adult pigs: P= 0.004). Neonatal humans and pigs had similar clottability (P= 0.989) values as did adult samples (P= 0.995).

Analysis of clot architecture:

We first examined and contrasted the fibrin clot structure with confocal microscopy between adult and neonatal porcine samples as a function of thrombin concentration (Figure 3). In general, adult porcine clots were denser and more heavily branched with increasing fiber density with increasing thrombin concentration. Fiber density is calculated as the ratio of black pixels (fibers) over white pixels (blank space), therefore this measurement is unitless.

Conversely, neonatal porcine fibrin clots were more aligned with a lower fiber density compared to adults (alignment index values: neonatal pigs 0.1, 0.25, and 0.5 U/mL thrombin: 1.12 +/− 0.05, 1.18 +/− 0.08, 1.15 +/− 0.09; adult pigs 0.1, 0.25, 0.5 U/mL thrombin: 1.07 +/− 0.006, 1.08 +/− 0.05, 1.07 +/− 0.07, 0.1 U/mL thrombin: neonatal pigs vs. adult pigs $P = 0.814$, 0.25 U/mL thrombin: neonatal pigs vs. adult pigs $P = 0.063$, 0.5 U/mL thrombin: neonatal pigs vs. adult pigs $P = 0.196$; fiber density: neonatal pigs 0.1, 0.25, 0.5 U/mL thrombin: 0.23+/− 0.19, 0.25+/− 0.29, 0.54 +/− 0.16; adult pigs 0.1, 0.25, 0.5 U/mL thrombin: 0.56 +/− 0.21, 1.19 +/− 0.72, 1.27 +/− 0.36, 0.1 U/mL thrombin: neonatal pigs vs. adult pigs $P = 0.801$, 0.25 U/mL thrombin: neonatal pigs vs. adult pigs $P = 0.026$, 0.5 U/mL thrombin: neonatal pigs vs. adult pigs $P = 0.118$). For all subsequent structural analyses, a thrombin concentration of 0.5 U/mL was utilized. We also examined and contrasted fibrin clot structure with cryogenic scanning electron microscopy between neonatal and adult porcine samples (Supplemental Figure 2). Three-dimensional structure reflected similar structural patterns identified via confocal microscopy with neonatal porcine samples more highly aligned compared to the densely-branched network in adult porcine clots. However, because the freezing technique required for cryogenic scanning electron microscopy may impact clot porosity, it was utilized as a secondary method of image analysis and did not include quantitative analysis. Next, we utilized confocal microscopy to examine fibrin clot architecture across species (Figure 4). In general, age-related structural relationships were consistent across species. Neonatal porcine and human clots exhibited minimally branched, aligned, sheet-like fibrin matrices with significantly lower fiber densities than the adult groups (neonatal humans: 0.61 +/− 0.28, neonatal pigs: 0.54 +/− 0.16, adult humans: 1.41 +/− 0.5, adult pigs: 1.27 +/− 0.36 black/white pixels, neonatal humans vs. adult humans $P = 0.043$, neonatal pigs vs. adult pigs $P = 0.035$, neonatal human vs. neonatal pigs $P = 0.903$, adult human vs. adult pigs $P=0.938$). Neonatal human and porcine samples resulted in higher clot fiber alignment values than adult humans or pigs (neonatal humans: 1.22 +/− 0.09, neonatal pigs: 1.14 +/− 0.07, adult humans: 1.09 +/− 0.02, adult pigs: 1.07 +/− 0.02; neonatal humans vs. adult humans: $P = 0.021$, neonatal pigs vs. adult pigs: $P = 0.051$, neonatal human vs. neonatal pigs: $P= 0.092$, adult human vs. adult pigs: $P=0.795$).

Analysis of clot stiffness:

Fibrin clot mechanical properties were evaluated via atomic force microscopy nano indentation. Force maps were generated (Supplemental Figure 3) and average stiffness values are shown in Figure 5. We observed statistically significant lower clot stiffness values in neonatal human plasma clots compared to adults. These tendencies were mirrored in porcine samples (neonatal humans: 1.60 +/− 0.18, neonatal pigs: 1.40 +/− 1.1, adult humans: 4.3 +/− 0.95, adult pigs: 4.3 +/− 0.96 kPa; neonatal humans vs. adult humans: $P = 0.016$, neonatal pigs vs. adult pigs: $P = 0.015$, neonatal human vs. neonatal pigs: $P > 0.999$, adult human vs. adult pigs: $P > 0.999$).

Analysis of clot degradation:

A custom microfluidics assay was utilized to determine plasma clot degradation rates (Figure 6)[7]. Clots formed from neonatal human and pig plasma samples had significantly faster rates of degradation compared to adult human and pig groups (Neonatal humans: 24.9

+/− 4.9, neonatal pigs: 32.6 +/− 5.2, adult humans: 13.9 +/− 3.1, adult pigs: 12.4 +/− 4.1 μm/hour; neonatal humans vs. adult humans: $P = 0.048$, neonatal pigs vs. adult pigs: $P < 0.0001$, neonatal human vs. neonatal pigs: $P = 0.140$, adult human vs. adult pigs: $P = 0.969$).

Analysis of pro-coagulants in porcine model of hemodilution:

Neonatal porcine plasma was diluted to model the dilutional coagulopathy and associated reduction in fibrinogen seen after CPB[7]. Confocal microscopy was utilized to examine clot structure with or without the addition of factor VIIa, FEIBA, RiaSTAP, or platelet-like particles (Figure 7). Clots constructed of diluted porcine plasma were porous and heterogeneous in structure. The addition of all hemostatic therapies enhanced formation of the fibrin network with more complete fibrin matrices. The addition of platelet-like particles to diluted porcine plasma resulted in clots with statistically significant higher fiber density values (diluted plasma: 0.22 +/− 0.17, factor VIIa: 0.31 +/− 0.12, FEIBA: 0.61 +/− 0.29, RiaSTAP: 0.57 +/− 0.19, PLPs: 0.83 +/− 0.40, diluted vs. factor VIIa $P = 0.989$, diluted vs. FEIBA $P = 0.122$, diluted vs. RiaSTAP $P = 0.199$, diluted vs. PLPs $P = 0.005$). Clot fiber alignment in the presence of factor VIIa was similar to control. The addition of FEIBA and platelet-like particles resulted in decreased, although not statically significant, alignment values (diluted plasma: 1.13 +/− 0.09, factor VIIa: 1.16 +/− 0.08, FEIBA: 1.06 +/− 0.01, RiaSTAP: 1.02 +/−0.10 PLPs: 1.06 +/− 0.01, diluted vs. factor VIIa $P = 0.989$, diluted vs. FEIBA $P = 0.340$, diluted vs. RiaSTAP $P = 0.886$, diluted vs. PLPs $P = 0.402$). Next, clottability was determined for diluted neonatal plasma with and without the addition of procoagulants. Diluted neonatal porcine plasma clots had a lower average clottability (47 +/− 31 %) than those formed from factor VIIa (66 +/− 24 %, FEIBA: 79 +/− 20%, RiaSTAP: 86 +/− 6%, or PLPs 88 +/− 8%, diluted vs. factor VIIa $P = 0.225$, diluted vs. FEIBA $P = 0.126$, diluted vs. RiaSTAP $P = 0.039$, diluted vs. PLPs $P = 0.047$).

Discussion:

Our results show that age-related differences identified in human fibrinogen are mirrored in pigs, thus confirming piglets as an appropriate preclinical model to evaluate the effects of neonatal specific hemostatic therapies on the fibrin network. To determine this, we thoroughly analyzed several aspects of fibrinogen and its resultant fibrin network across both species. We found that fibrinogen concentration and functionality in plasma collected from piglets accurately parallels those observed in plasma collected from human neonates. Fibrin network structure, when analyzed via confocal and cryogenic scanning electron microscopy, also displayed similar tendencies with highly aligned fibrin networks in both neonatal species compared to highly branched networks in adults. Lastly, we assessed fibrin network stiffness and degradation patterns between neonates and adults in both species and again found substantial similarities. To assess a potential application, post-CPB coagulopathy, we analyzed the structural and functional effects of several pro-coagulant therapies on the fibrin network formed from diluted piglet plasma. We found that the *ex vivo* addition of factor VII, FEIBA, RiaSTAP, and platelet-like particles augmented fibrin network properties as seen in our prior studies performed with human neonatal plasma obtained after CPB[17,18].

Coagulopathy can considerably complicate the clinical management of neonatal patients and results in significant morbidity and mortality[4]. It is frequently seen during major surgery, extracorporeal membrane oxygenation and sepsis. When these patients require surgical treatment, anesthesiologists are presented with a challenging situation. Although our understanding of the importance of fibrinogen replacement in the treatment of severe bleeding has improved over recent years, available options to replenish it have not. The effectiveness of fresh frozen plasma to restore fibrinogen is poor due to a lack of potency, and the large volumes required in a neonate make it an impractical solution. Cryoprecipitate is more effective in providing higher concentrations of fibrinogen but shares similar disadvantages to fresh frozen plasma: fibrinogen concentration is variable, blood group matching in neonates is recommended, time is required for thawing and there is a risk of viral transmission. For those reasons cryoprecipitate is not available in several countries. Fibrinogen concentrate (RiaSTAP; CSL Behring, USA), made from pooled human plasma, is increasingly being used to replete fibrinogen, but has limited availability and represents yet another form of adult fibrinogen which may not be compatible in the neonatal system[4,7,24]. Progress towards discovering improved methods to treat neonatal coagulopathy have been hindered by an inadequate understanding of the differences between adult and neonatal hemostasis, few well-performed clinical studies evaluating therapies to treat bleeding in neonates, and lack of a validated animal model of neonatal coagulopathy. Our results represent a step towards this important goal.

To assess developmental similarities between human and porcine fibrinogen, we conducted a series of analyses comparing function, structure and degradation between adult and neonatal human and porcine fibrin networks. To analyze the functionality of fibrinogen between species, we assessed clottability for all sample groups and found statistically significantly lower clottability values in human neonatal fibrinogen than in adult fibrinogen. This same relationship was reflected in the porcine samples. Structurally, we observed a three-dimensional, highly branched clot architecture in adult porcine samples verses thin, sheet-like fibrin matrices with little cross branching in neonatal porcine samples. Our quantitative analysis also revealed higher alignment and lower fiber density in neonatal porcine samples compared to adults. At a thrombin concentration of 0.5 U/mL, we performed a comparative image analysis with human samples and again identified similar structural differences between age groups in pigs and humans. Both neonatal species exhibited fibrin clots with a higher degree of alignment and statistically significant lower fiber densities when compared to corresponding adult clots. Moreover, these structural differences agree with our previous data examining fibrin clot structure constructed from neonatal and adult purified fibrinogen[7]. We speculate that these structural differences are the result of differences in fibrin polymerization. Future studies are necessary to elucidate the underlying mechanisms.

Our model validation also included analysis of human and porcine clot mechanical properties. Research has linked structurally dense, highly branched clots to greater clot stiffness[25,26]. Here, we used atomic force microscopy to measure plasma clot stiffness in both porcine and human samples. We found clots formed from neonatal human plasma had statistically significantly lower average stiffness values than those formed from adult human plasma ($P = 0.016$). These patterns were mirrored in clots formed from neonatal and adult porcine samples ($P = 0.015$).

In addition to polymerization rates, an accurate animal model must also display a fibrinolytic potential similar to humans. Thus, we measured degradation rates between age groups and species using a custom microfluidic device. We identified statistically significantly faster plasma degradation rates in neonatal samples compared to adults. Previous research has indicated that fibrinolysis is related to clot structure where denser, heavily branched clots have slower degradation rates than more porous clots[27,28]. Our data agrees with this relationship in that both neonatal porcine and human plasma clots exhibited rapid rates of degradation and lower fiber densities when compared to adult samples. This data is also consistent with our previous work where we identified statistically significant faster rates of fibrin clot degradation in neonates compared to adults, and when mixed together (to simulate transfusion with cryoprecipitate), clot degradation was statistically significant slower than baseline neonatal rates[7]. We hypothesize that the intrinsic neonatal fibrinolytic system may not properly degrade adult fibrinogen and thus contributing to the high rate of thrombotic complications observed in neonates after cardiac surgery[29]. It is imperative that potential hemostatic therapies for surgical procedures be balanced to augment clotting while simultaneously limiting thrombotic complications. A valid preclinical animal model would aid this objective. Anti-fibrinolytic therapy is often used before, during, and post-CPB to reduce bleeding by inhibiting degradation but its clinical efficacy in the neonatal population is inconsistent[30].

After validation of our model, we next focused on its potential application as an *in vitro* model for post-CPB hemodilution. We diluted neonatal porcine plasma to mimic the reduction in clotting fibrinogen seen after CPB. Structural analysis of these samples revealed very porous clot architecture with low clottability (Figure 7), and emulate our previous experiments characterizing post-CPB clots made from neonatal plasma[7,18]. Next, to explore possible treatment options for post-CPB bleeding, novel and commercially available hemostatic therapeutics were applied to the diluted samples. Structurally, all therapeutics enhanced fibrin clot formation and resulted in more complete fibrin matrices. Additionally, the addition of synthetic platelet-like particles to diluted plasma produced in a statistically significant increase in fiber density. Again, the results from these structural analyses are in line with our previous studies demonstrating that the *ex vivo* addition of factor VIIa, FEIBA, RiaSTAP and platelet like particles to post-CPB human neonatal plasma augment fibrin network porperties[17,18]. Future studies should include a thorough analysis of degradation rates within the neonatal system.

This study has several limitations. First, our experiments are conducted *ex vivo* with either purified fibrinogen or plasma and therefore may not accurately represent *in vivo* physiology. Specifically, our experiments did not account for the complexity of whole blood, including the crucial role of platelets in hemostasis. Future studies using whole blood samples and/or platelet-rich-plasma are essential to better investigate the intricacy of *in vivo* coagulation and fibrinolytic responses. However, the simplified system utilized in our study allowed for the detailed focus on age dependent differences in fibrinogen and plasma fibrin networks between humans and pigs. Also, due to the accelerated timeline of ageing in pigs compared to humans, it is likely the eight week old piglets used in this study do not accurately reflect the neonatal period in humans. The samples utilized in this study were obtained based on availability from North Carolina State University's School of Veterinary Medicine. Follow

up studies should include an analysis of younger porcine plasma samples to allow for more precise age matching between species. None-the-less, we show that 8 week old piglets could serve as a useful preclinical model of human neonatal fibrin deficiencies. Also, using 8 week old piglets is logistically easier than very young, newborn pigs as they are already weaned. Additionally, all sample groups utilized in this study included both male and female samples except for the adult porcine group in which there were only females. The experiments in this study have not been explored on the basis of sex and therefore it is possible that the addition of male pigs in the adult porcine group may alter results. This study utilized plasma samples from healthy piglets in order to establish a baseline *in vitro* model. However, the presence of congenital heart defects may add complexity to the coagulation system from poor circulation and cyanosis. Some porcine models of severe congenital heart disease, including tetralogy of Fallot, have been described[31]. In future research, porcine models with congenital heart defects should be used for *in vitro* characterization of plasma samples and *in vivo* analysis of bleeding to identify potential discrepancies between noncardiac neonatal piglets and piglets with complex congenital heart disease. Finally, the coagulopathy that results from CPB in neonates is complex and involves consumptive processes as well. Here, we concentrated only on the hemodilutional aspect of bypass induced coagulopathy. However, focusing on the reduction in fibrinogen allowed us to examine the effect of procoagulants on fibrin properties in a less complicated system. While informative, future studies should expose neonatal piglets to CPB and subsequently characterize clotting properties.

In summary, our results validate that piglets can serve as an appropriate animal model capable of reflecting the developmental nuances observed in human fibrinogen. Recent evidence confirms that neonatal fibrinogen is qualitatively distinct from adult fibrinogen resulting in differences between neonatal and adult fibrin clot structure. In our analyses, we observed similar fibrinogen concentrations and clottability across species as well as similar age-related patterns in structure, mechanical, and degradation properties of adult and neonatal porcine and human samples. Based on these results we conclude that piglets are indeed an appropriate preclinical animal model for neonatal hemostasis. In addition, we demonstrated the feasibility of an *in vitro* model application through the analysis of several hemostatic therapies applied to diluted neonatal porcine plasma.

Supplementary Material

Refer to Web version on PubMed Central for supplementary material.

Acknowledgements:

Work Cited:

1. Andrew M, Paes B, Milner R, Johnston M, Mitchell L, Tollefsen DM, Castle V, Powers P: Development of the human coagulation system in the healthy premature infant. Blood 1988; 72:1651–7 [PubMed: 3179444]

2. Ignjatovic V, Mertyn E, Monagle P: The coagulation system in children: developmental and pathophysiological considerations. Semin Thromb Hemost 2011; 37:723–9 [PubMed: 22187394]

3. Toulon P: Developmental hemostasis: laboratory and clinical implications. Int J Lab Hematol 2016; 38 Suppl 1:66–77 [PubMed: 27426861]

4. Guzzetta NA, Allen NN, Wilson EC, Foster GS, Ehrlich AC, Miller BE: Excessive postoperative bleeding and outcomes in neonates undergoing cardiopulmonary bypass. Anesth Analg 2015; 120:405–10 [PubMed: 25390280]

5. Guzzetta NA: Benefits and risks of red blood cell transfusion in pediatric patients undergoing cardiac surgery. Paediatr Anaesth 2011; 21:504–11 [PubMed: 21114707]

6. Guzzetta NA, Williams GD: Current use of factor concentrates in pediatric cardiac anesthesia. Paediatr Anaesth 2017; 27:678–87 [PubMed: 28393462]

7. Brown AC, Hannan R, Timmins LH, Fernandez JD, Barker TH, Guzzetta NA: Fibrin network changes in neonates after cardiopulmonary bypass. Anesthesiology 2016; 124:1021–31 [PubMed: 26914227]

8. Ignjatovic V, Lai C, Summerhayes R, Mathesius U, Tawfilis S, Perugini MA, Monagle P: Age-Related Differences in Plasma Proteins: How Plasma Proteins Change from Neonates to Adults. PLOS ONE 2011; 6:e17213 [PubMed: 21365000]

9. Ignjatovic V, Ilhan A, Monagle P: Evidence for age-related differences in human fibrinogen. Blood Coagul Fibrinolysis Int J Haemost Thromb 2011; 22:110–7

10. Münster A-MB, Olsen AK, Bladbjerg E-M: Usefulness of human coagulation and fibrinolysis assays in domestic pigs. Comp Med 2002; 52:39–43 [PubMed: 11900411]

11. Olsen KA, Hansen AK, Jespersen J, Markmann P, Bladbjerg EM: The Pig as a model in blood coagulation and fibrinolysis research. Scand J Lab Anim Sci 1999; 26:214–25

12. Zentai C, Braunschweig T, Rossaint R, Daniels M, Czaplik M, Tolba R, Grottke O: Fibrin patch in a pig model with blunt liver injury under severe hypothermia. J Surg Res 2014; 187:616–24 [PubMed: 24332553]

13. Inaba K, Barmparas G, Rhee P, Branco BC, Fitzpatrick M, Okoye OT, Demetriades D: Dried Platelets in a Swine Model of Liver Injury: Shock 2014; 41:429–34 [PubMed: 25133601]

14. Greek R, Rice MJ: Animal models and conserved processes. Theor Biol Med Model 2012; 9:40 [PubMed: 22963674]

15. Zeng L, Choonara I, Zhang L, Li Y, Shi J: Effectiveness of prothrombin complex concentrate (PCC) in neonates and infants with bleeding or risk of bleeding: a systematic review and meta-analysis. Eur J Pediatr 2017; 176:581–9 [PubMed: 28281092]

16. Hedner U, Erhardtsen E: Potential role for rFVIIa in transfusion medicine. Transfusion (Paris) 2002; 42:114–24

17. Brown AC, Stabenfeldt SE, Ahn B, Hannan RT, Dhada KS, Herman ES, Stefanelli V, Guzzetta N, Alexeev A, Lam WA, Lyon LA, Barker TH: Ultrasoft microgels displaying emergent platelet-like behaviours. Nat Mater 2014; 13:1108–14 [PubMed: 25194701]

18. Nellenbach K, Guzzetta NA, Brown AC: Analysis of the structural and mechanical effects of procoagulant agents on neonatal fibrin networks following cardiopulmonary bypass. J Thromb Haemost JTH 2018; 16:2159–67 [PubMed: 30182421]

19. Nandi S, Sproul EP, Nellenbach K, Erb M, Gaffney L, Freytes DO, Brown AC: Platelet-like particles dynamically stiffen fibrin matrices and improve wound healing outcomes. Biomater Sci 2018 doi:10.1039/C8BM01201F

20. Nandi S, Brown AC: Platelet-mimetic strategies for modulating the wound environment and inflammatory responses. Exp Biol Med Maywood NJ 2016; 241:1138–48

21. Sproul E, Hannan R, Brown AC: Characterization of fibrin-based constructs for tissue engineering, Methods in Molecular Biology-Biomaterials. New York, Springer, 2018.

22. Timmins LH, Wu Q, Yeh AT, Moore JE, Greenwald SE: Structural inhomogeneity and fiber orientation in the inner arterial media. Am J Physiol Heart Circ Physiol 2010; 298:H1537–1545 [PubMed: 20173046]

23. Spiess BD, Armour S, Horrow JC, Kaplan JA, Koch C, Karkouti K, Body SC: Transfusion Medicine and Coagulation Disorders 2017 doi:10.1016/B978-0-323-49798-5.00027-9

24. Williams GD, Bratton SL, Ramamoorthy C: Factors associated with blood loss and blood product transfusions: a multivariate analysis in children after open-heart surgery. Anesth Analg 1999; 89:57–64 [PubMed: 10389779]

25. Undas A, Ariëns RAS: Fibrin clot structure and function: a role in the pathophysiology of arterial and venous thromboembolic diseases. Arterioscler Thromb Vasc Biol 2011; 31:e88–99 [PubMed: 21836064]

26. Weisel JW: Structure of fibrin: impact on clot stability: Structure of fibrin: impact on clot stability. J Thromb Haemost 2007; 5:116–24 [PubMed: 17635717]

27. Weisel JW, Litvinov RI: The biochemical and physical process of fibrinolysis and effects of clot structure and stability on the lysis rate. Cardiovasc Hematol Agents Med Chem 2008; 6:161–80 [PubMed: 18673231]

28. Undas A: Prothrombotic Fibrin Clot Phenotype in Patients with Deep Vein Thrombosis and Pulmonary Embolism: A New Risk Factor for Recurrence. Biomed Res Int 2017 doi:10.1155/2017/8196256

29. Manlhiot C, Menjak I, Brandao L, Gruenwald C, Schwartz S, Sivarajan V, Yoon H, Maratta R, Carew C, McMullen J, Clarizia N, Holtby H, Williams S, Caldarone C, Van Arsdell G, Chan A, McCrindle B: Risk, Clinical Features, and Outcomes of Thrombosis Associated with Pediatric Cardiac Surgery. Circulation 2011; 124:1511–9 [PubMed: 21911785]

30. Stayer SA, Mossad EB, Miller-Hance WC :Anesthesia for Congenital Heart Disease. John Wiley & Sons, 2015.

31. Camacho P, Fan H, Liu Z, He J-Q: Large Mammalian Animal Models of Heart Disease. J Cardiovasc Dev Dis 2016; 3:30
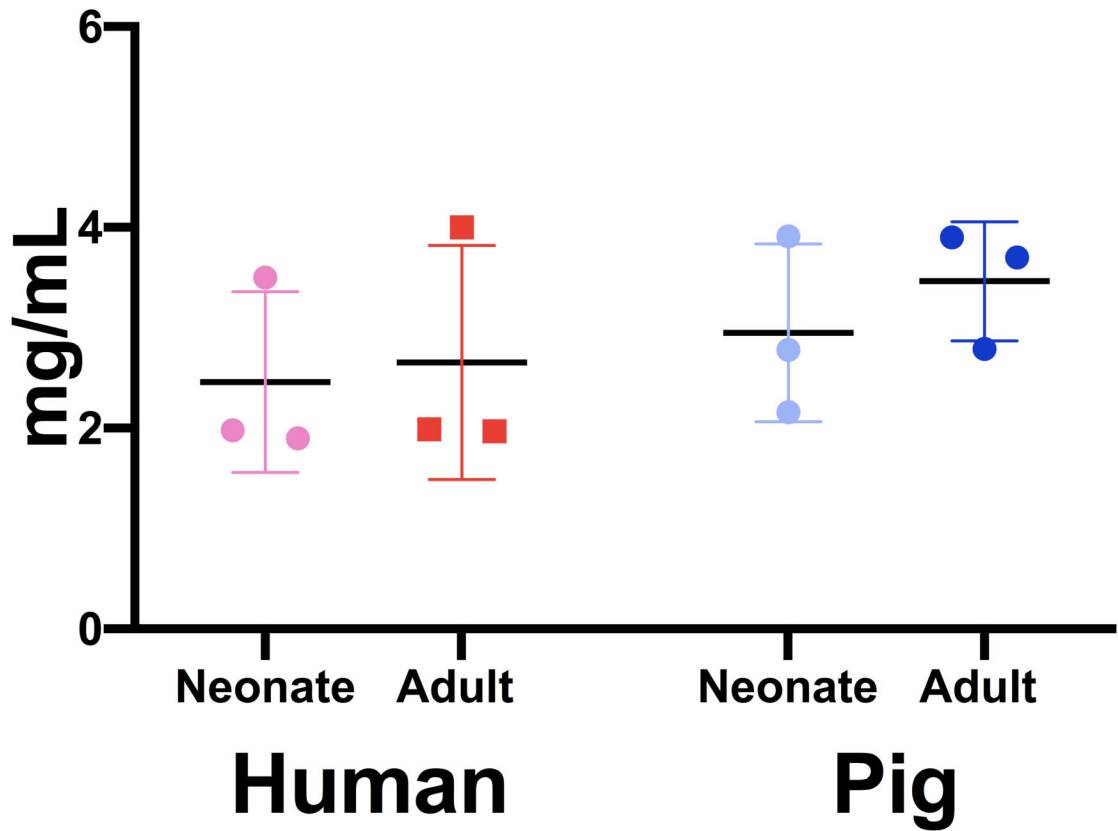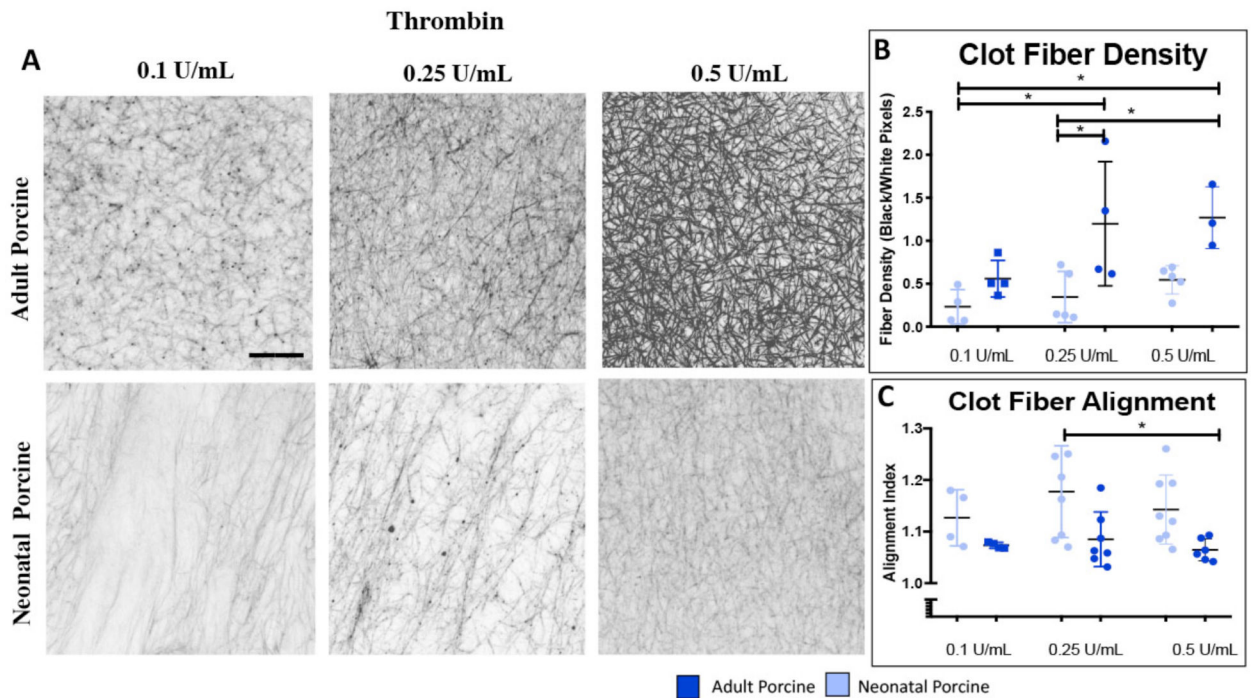
Figure 1.
Quantification of fibrinogen levels in platelet poor plasma. Fibrinogen was quantified via ELISA across species and age ranges. Average fibrinogen concentrations +/− standard deviation is shown. N=3.
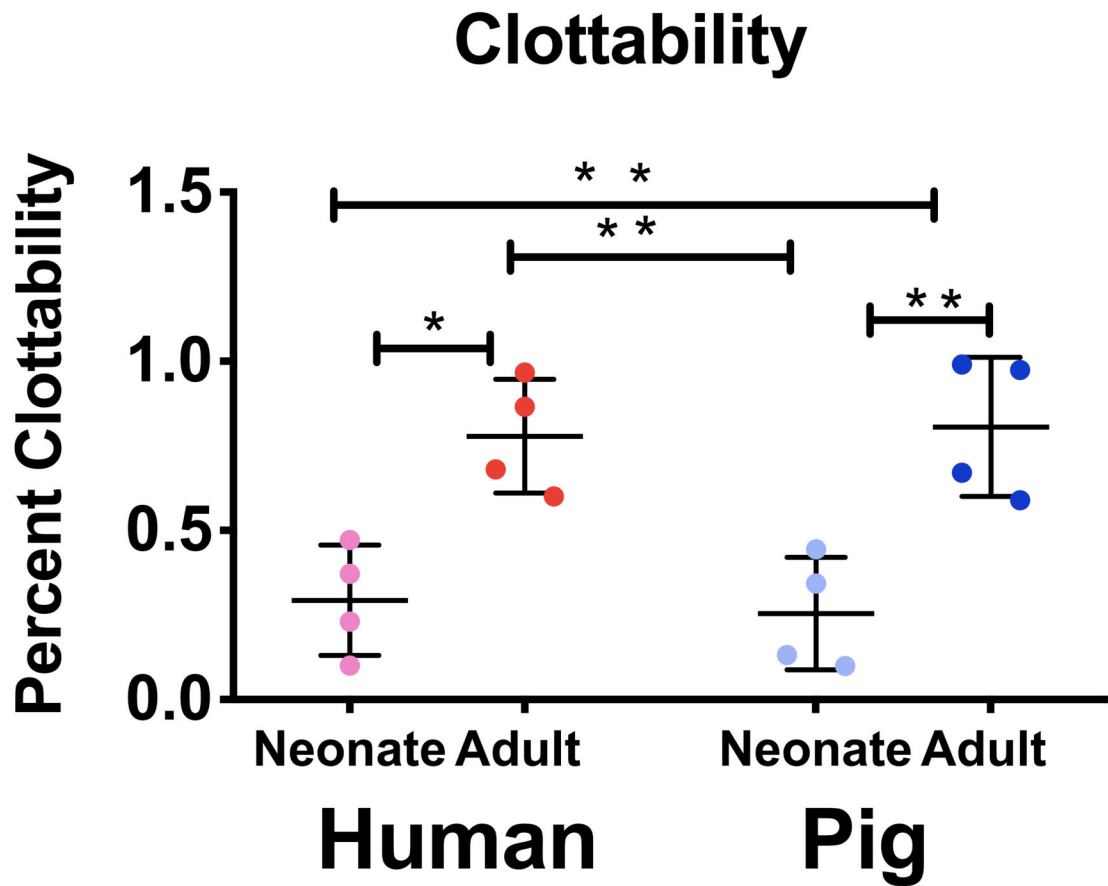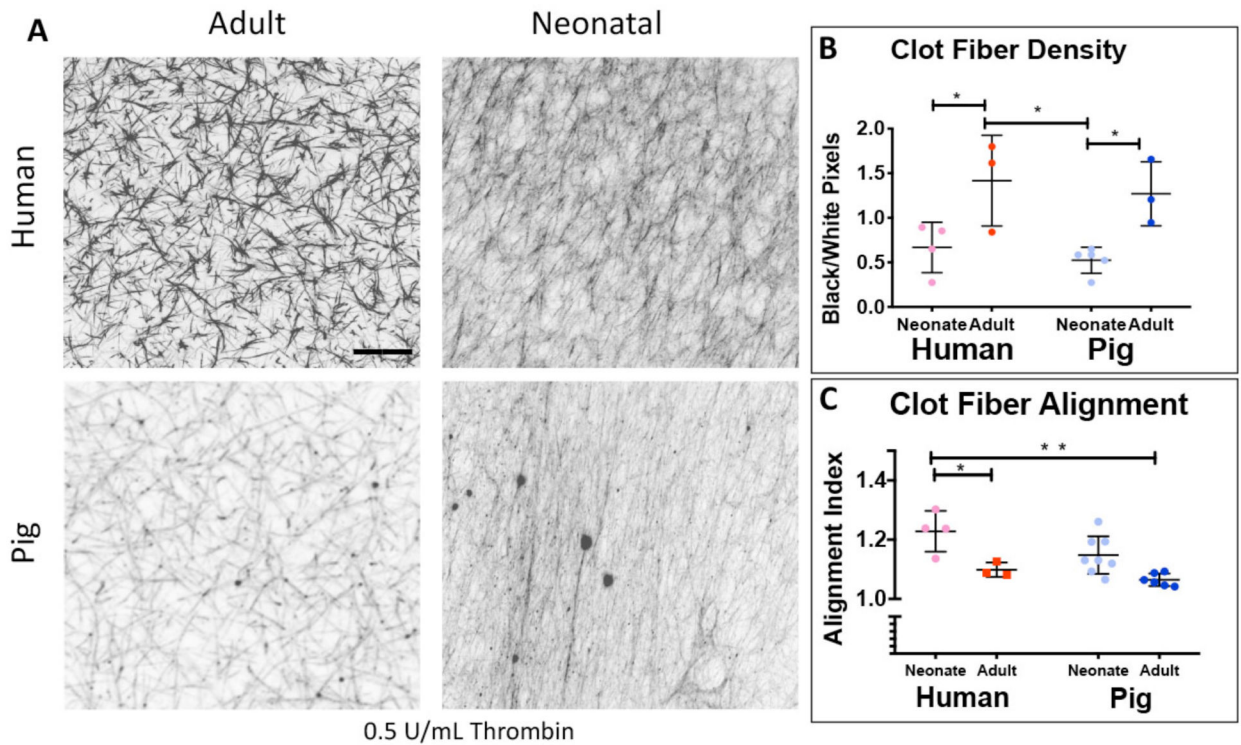
Figure 2.
Quantification of isolated fibrinogen clottability across species. Clottability of purified fibrinogen was determined via NanoOrange Protein Quantification Kit. Average clottability +/− standard deviation is reported. N=4 *p<0.05, **p<0.01
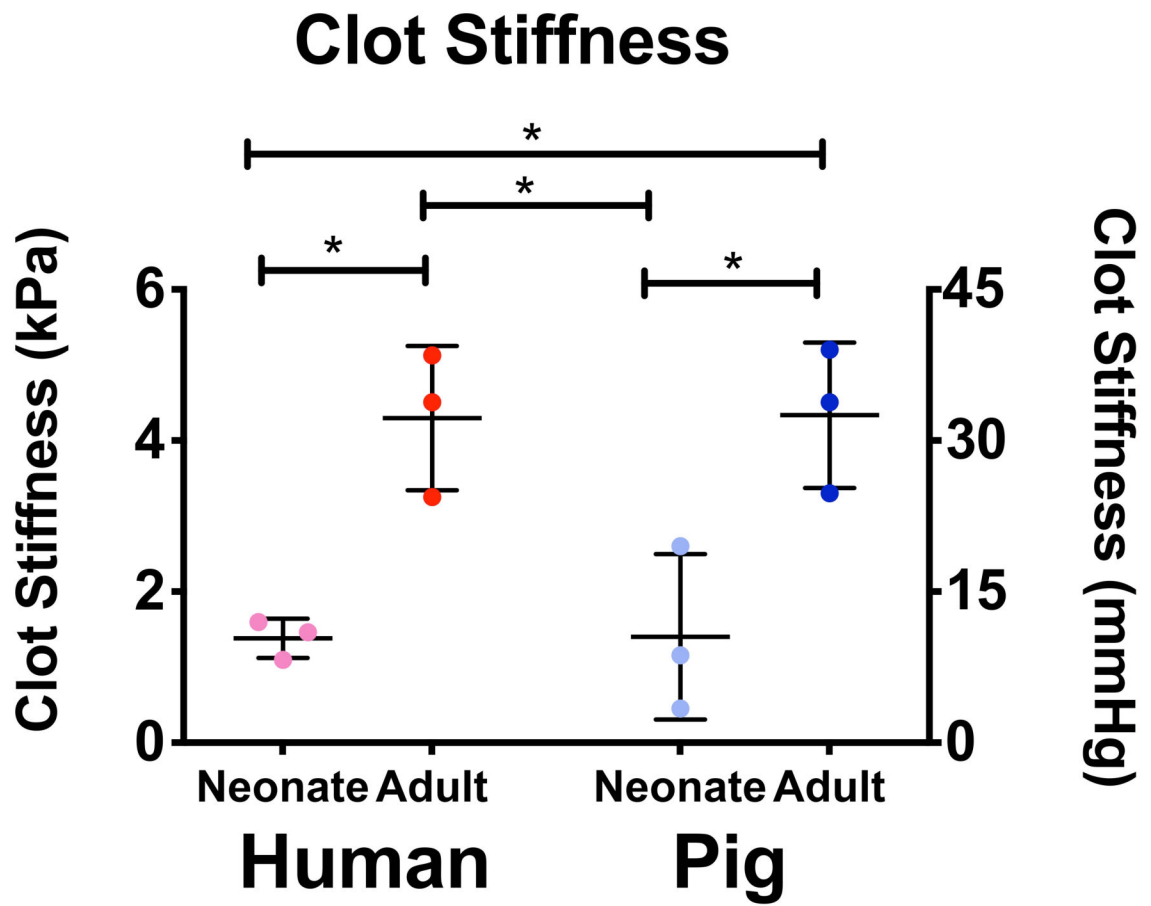
Figure 3.
Confocal microscopy analysis of structure of adult and neonatal porcine clots formed with increasing thrombin (A). Average clot fiber alignment (B) and fiber density (C) +/− standard deviation are shown. 0.1 U/mL Thrombin: neonatal pigs N=4, adult pigs N=4, 0.25 U/mL Thrombin: neonatal pigs: N=8, adult pigs N=7, 1.0 U/mL Thrombin: neonatal pigs: N=8, adult pigs N=6. *p<0.05.
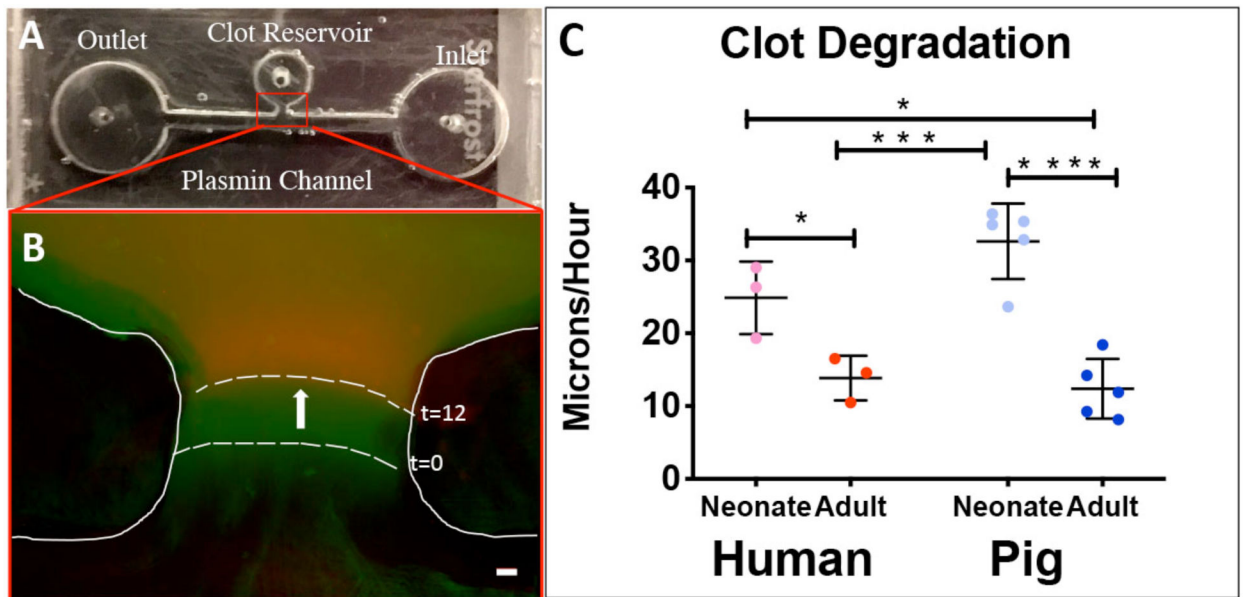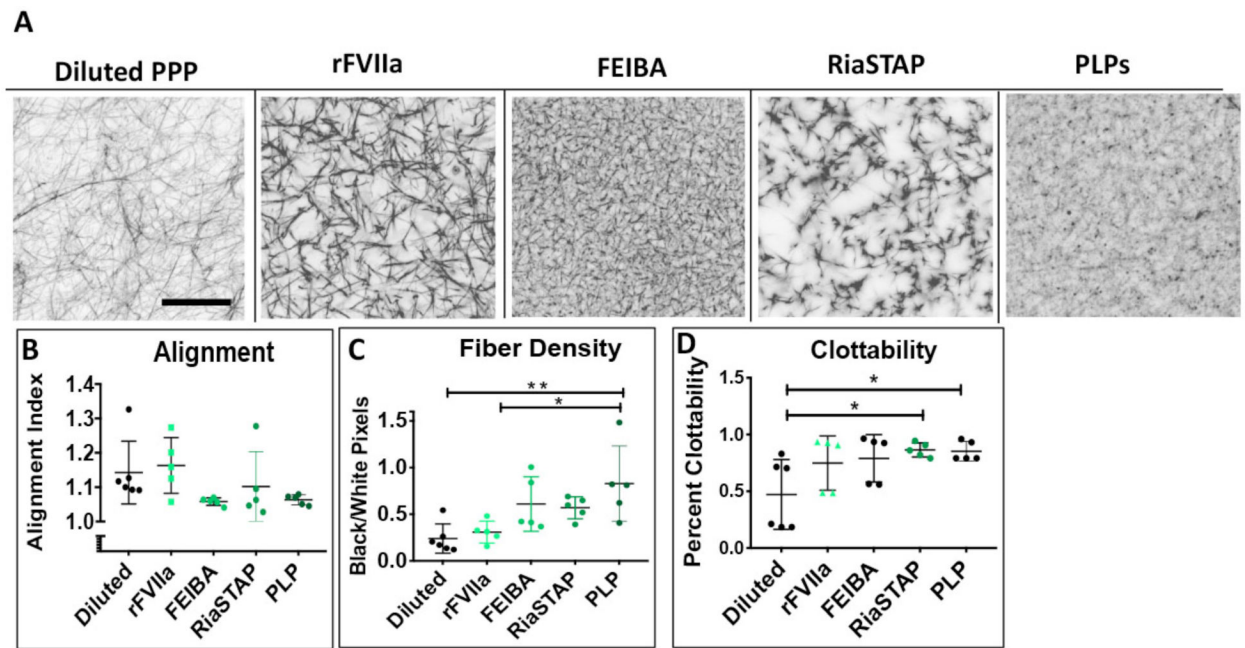
Figure 4.
Confocal microscopy analysis of structure of adult and neonatal human and porcine clots formed with 0.5 U/mL Thrombin (A). Average clot fiber alignment (B) and fiber density (C) +/− standard deviation is shown. Alignment: neonatal humans: N=4, adult humans: N=3, neonatal pigs: N=8, adult pigs: N=6. Fiber Density: neonatal humans: N=4, adult humans: N=3, neonatal pigs: N=5, adult pigs: N=3. *p<0.05, **p<0.01.

Figure 5.
Atomic force microscopy analysis of plasma clot stiffness across species. Mean stiffness +/−
standard deviation is shown. N=3; *p<0.05.

Figure 6.
Evaluation of plasma clot degradation with a custom microfluidic device. Top view of the device (A). Initial (green) and final (red) frames of clot boundary overlaid with false coloring (B). Average Degradation rates +/− standard deviation. neonatal humans: N=3, adult humans: N=3, neonatal pigs: N=5, adult pigs: N=5. Scale = 10 μm. *p<0.05, **p<0.01, ***p<0.001, ****p<0.0001.

Figure 7.
Structural and functional analysis of hemostatic agents in diluted neonatal porcine plasma. Representative images are shown of diluted neonatal porcine plasma in the absence or presence of FEIBA, factor VII (rFVIIa), or platelet-like particles (PLPs) (A). Average clot fiber density (B), alignment (C), and clottability (D) are reported +/− standard deviation. Structural analysis: plasma: N=7, FEIBA, factor VII, RiaSTAP, platelet-like particles: N=5. Clottability: platelet poor plasma: N=6, FEIBA, factor VII, RiaSTAP, platelet-like particles: N= 5 *p<0.05, **p<0.01.